

Crossover of aging dynamics in polymer glass: From cumulative aging to noncumulative aging

K. Fukao* and S. Yamawaki

Department of Polymer Science, Kyoto Institute of Technology, Matsugasaki, Kyoto 606-8585, Japan

(Received 17 January 2007; revised manuscript received 17 May 2007; published 24 August 2007)

The aging behavior of polymer glass, poly(methyl methacrylate), has been investigated through the measurement of the ac-dielectric susceptibility at a fixed frequency after a temperature shift ΔT (≤ 20 K) between two temperatures T_1 and T_2 . A crossover from cumulative aging to noncumulative aging could be observed with increasing ΔT using a twin-temperature (T -) shift measurement. Based on the growth law of a dynamical coherent length given by activated dynamics, we obtain a unique coherent length for positive and negative T shifts. The possibility of the existence of temperature chaos in polymer glasses is discussed.

DOI: 10.1103/PhysRevE.76.021507

PACS number(s): 64.70.Pf, 77.84.Jd, 75.50.Lk

I. INTRODUCTION

In amorphous materials, a glass transition is observed when the temperature decreases from a high temperature in a liquid state to a lower temperature. Below the glass transition temperature T_g , the structure of amorphous materials is disordered and the mobility due to a primary motion, which is usually called the α process, is lost. Thus, the system is in a *glassy state*. However, even in the glassy state, there is a very slow relaxation toward an equilibrium state [1,2]. This slow relaxation is called aging and is regarded as an important common property characteristic of disordered materials, such as spin glasses [3–6], orientational glasses [7], supercooled liquids [8], relaxor ferroelectrics [9], and polymer glasses [10,11]. Among the most interesting phenomena observed in the aging behavior are *memory and rejuvenation* effects [6]. The elucidation of these effects is essential for understanding the aging dynamics in glassy states and also the nature of the glass transition.

In our previous papers, we reported that the dielectric susceptibility of polymer glasses, poly(methyl methacrylate) (PMMA) [12], and polystyrene (PS) [13] shows memory and rejuvenation effects during an aging process below T_g . In these measurements, the system was quenched from a temperature above T_g to an initial temperature T_1 , at which the system is aged for time t_1 . The temperature is then shifted to a lower temperature T_2 ($=T_1 - \Delta T$) and maintained at this temperature for time t_2 . The temperature is then returned to and maintained at T_1 . Although in the first stage at T_1 the imaginary part of the ac-dielectric susceptibility $\epsilon''(\omega; t_w)$ decreases with increasing aging time t_w (referred to as *aging*), it increases to a higher value and then begins to decrease again just after the temperature is shifted to T_2 . This behavior is called *rejuvenation*. If ΔT is large enough, the relaxation of dielectric susceptibility, which restarts at time $t_w = t_1$, is approximately the same as that observed just after quenching directly from a high temperature ($> T_g$) to T_2 . Furthermore, at time $t_w = t_1 + t_2$, the value of the dielectric susceptibility returns to the value that $\epsilon''(\omega; t_w)$ had reached at time $t_w = t_1$ and then begins to decrease as if the system had not experi-

enced the lower temperature T_2 . This is called the *perfect memory effect*. The memory and rejuvenation effects are also observed in the real part of the ac susceptibility ϵ' for PMMA. It should be noted that the memory and rejuvenation effects on ϵ' and ϵ'' observed in polymer glasses are quite similar to those observed for ac-magnetic susceptibility $\chi''(\omega; t_w)$ in spin-glass systems, although there is a large difference in structure between polymeric materials and spin glass. Therefore, it is thought that there is a universal physical phenomenon related to this aging behavior.

II. CUMULATIVE AND NONCUMULATIVE AGING

An important concept for understanding glassy dynamics including memory and rejuvenation effects is the correlation length $\ell_T(t_w)$ after aging for time t_w at temperature T . This quantity was originally introduced to describe the spin-spin correlation in the spin-glass phase [2,14]. In the present case, in which the dielectric susceptibility $\epsilon''(\omega; t_w)$ of polymers is discussed, we can assume that the correlation length $\ell_T(t_w)$ describes the spatial correlation of dipole moments attached to the polymer chains. In this case, the correlation length $\ell_T(t_w)$ suggests that there is an ordered domain with a characteristic size of $\ell_T(t_w)$, where spins or dipole moments are aligned in an orderly manner.

Here, we consider a temperature-shift (T -shift) protocol, in which after the system is cooled down from a high temperature (above T_g) to T_1 (below T_g) and is aged at T_1 for time t_1 , the temperature is rapidly shifted to T_2 and is maintained at T_2 for time t_2 . This T -shift protocol is denoted as (T_1, T_2) . During the T -shift protocol, we measure $\epsilon''(\omega; t)$. We can then determine an effective time $t_{2,\text{eff}}$ such that the relation

$$\epsilon''(\omega; t_1 + t_w) = \epsilon''_{T_2}(\omega; t_{2,\text{eff}} + t_w) \quad (1)$$

is satisfied for any positive t_w , where ϵ''_{T_2} is the dielectric susceptibility obtained for an isothermal aging process at T_2 for an aging time $t_{2,\text{eff}} + t_w$. In practice, $t_{2,\text{eff}}$ is a fitting parameter and is obtained from the observed data. From this effective aging time, we can evaluate the effective correlation length ℓ_{eff} defined by the relation $\ell_{\text{eff}} \equiv \ell_{T_2}(t_{2,\text{eff}})$. In a *cumulative aging* scenario, we can expect that

*Present address: Department of Physics, Ritsumeikan University, Kusatsu, Shiga 525-8577 Japan. kfukao@se.ritsumeikan.ac.jp

$$\ell_{T_2}(t_{2,\text{eff}}) = \ell_{T_1}(t_1). \quad (2)$$

In this case, successive aging at the different temperatures T_1 and T_2 can be added in a totally cumulative manner, although the growth rate of the correlation length may depend on the aging temperature. Hence, the value of $t_{2,\text{eff}}$ and t_1 can be described by

$$t_{2,\text{eff}} = g(t_1, (T_1, T_2)), \quad t_1 = g^{-1}(t_{2,\text{eff}}, (T_1, T_2)),$$

where g is a function of t_1 , which depends on the choice of the initial and second temperatures T_1 and T_2 . Once a specific form of $\ell_T(t)$ is given, the form of g can be determined uniquely. In this case, there is a reversible aging between two temperatures. If this reversibility is violated, the aging is no longer cumulative, but rather it is *noncumulative*.

Here, we introduce a reverse T -shift protocol (T_2, T_1), where the system is aged at T_2 for time t_2 and the temperature then is shifted from T_2 to T_1 . For this protocol, we can obtain another effective aging time $t_{1,\text{eff}}$, which satisfies the relation

$$\epsilon'(\omega; t_2 + t_w) = \epsilon'_{T_1}(\omega; t_{1,\text{eff}} + t_w). \quad (3)$$

In the case of cumulative aging, we can also expect that

$$\ell_{T_1}(t_{1,\text{eff}}) = \ell_{T_2}(t_2). \quad (4)$$

In order to check whether the aging is cumulative or noncumulative, a *twin- T -shift experiment* has been proposed in the studies on spin glass by Jönsson, Yoshino, and Nordbald [15]. In the twin- T -shift experiment, a pair of T -shift experiments (T_1, T_2) and (T_2, T_1) are performed. Then, an effective aging time $t_{2,\text{eff}}$ [$t_{1,\text{eff}}$] is determined as a function of the aging time t_1 [t_2] at T_1 [T_2] for the T shift (T_1, T_2) [(T_2, T_1)], and the data points ($t_1, t_{2,\text{eff}}$) and ($t_{1,\text{eff}}, t_2$) for various values of t_1 and t_2 are plotted on the same plot, where the horizontal axis is t_1 or $t_{1,\text{eff}}$ and the vertical axis is $t_{2,\text{eff}}$ or t_2 , as shown in Fig. 4, below. If all data points fall onto a single curve, we can judge that the aging is cumulative. Otherwise, the aging is noncumulative.

In the present study, we have performed twin- T -shift experiments on the ac-dielectric susceptibilities during the aging process of PMMA glasses in order to check whether the aging dynamics is attributed to cumulative or noncumulative aging and also to check whether there is a crossover between these types. The present paper consists of six sections. After providing an explanation on cumulative aging in Sec. II and experimental details in Sec. III, experimental results on twin- T -shift measurements are presented in Secs. IV and V. Finally, a discussion of the experimental results is presented in Sec. VI.

III. EXPERIMENT

The polymer samples used in the present study are atactic PMMA purchased from Scientific Polymer Products, Inc. The weight-averaged molecular weight is $M_w = 3.56 \times 10^5$ and $M_w/M_n = 1.07$, where M_n is the number-averaged molecular weight. The glass transition temperature T_g determined by differential scanning calorimetry (DSC) is approxi-

mately 380 K. Thin films were prepared onto an aluminum vacuum-deposited glass substrate using the spin coat method from a toluene solution of PMMA. After annealing at 343 K, aluminum was vacuum deposited again to serve as an upper electrode. The thickness of the films used in the present study is 281 nm, as measured directly by atomic force microscopy. The preparation method of the above samples is the same as in our previous studies [16–18].

Dielectric measurements were performed using an LCR meter (HP4284A). The frequency range of the applied electric field was from 20 Hz to 1 MHz, and the applied voltage level was 2.0 V. In our measurements, the complex electric capacitance of the sample condenser C^* was measured and then converted into the ac-dielectric susceptibility ϵ^* by dividing C^* by the geometrical capacitance C_0 at a standard temperature T_0 . Here, C^* is given by $C^* = \epsilon^* \epsilon_0 \frac{S}{d}$ and $C_0 = \epsilon_0 \frac{S}{d}$, where ϵ_0 is the permittivity in vacuum, S is the area of the electrode, and d is the film thickness. For the evaluation of ϵ^* and C_0 , we use the thickness d given above and $S = 8 \times 10^{-6}$ m². The sample prepared above is located in a sample cell. The temperature of the sample cell is controlled through heaters wound along the outer surface of the sample cell. The temperature measured by a thermocouple attached to the backside of glass substrate is used as the temperature of the sample.

Heating cycles in which the temperature was varied between room temperature and 403 K ($>T_g$) were applied several times prior to the measurements in order to relax the as-prepared samples and obtain reproducible results. The relaxed sample is heated from room temperature to 403 K and then cooled to an aging temperature T_1 (T_2) at the rate of 0.5 K/min. The temperature is thereafter maintained at T_1 (T_2) for a time t_1 (t_2). The temperature is then changed to T_2 (T_1) at the rate of 0.5 K/min and is then maintained at T_2 (T_1) for 30 h. Here, the aging times t_1 and t_2 change from 1 h to 20 h. For the twin- T -shift measurements, during this thermal history, dielectric measurements between 1 MHz and 20 Hz are performed repeatedly. One measurement for this frequency range requires approximately 50 sec.

IV. DETERMINATION OF EFFECTIVE AGING TIMES

Figure 1 shows an example of the results observed for a positive T shift from $T_2 = 356.9$ K to $T_1 = 375.7$ K after aging at T_2 for a time $t_2 = 10$ h. The vertical axis is the real part of ac-dielectric susceptibility ϵ' relative to a reference value ϵ'_{ref} . The reference value for T_1 (T_2) is the value measured at T_1 (T_2) after direct quenching from 403 K to T_1 (T_2). Both values are measured at a fixed frequency of 100 Hz. Figure 1(a) shows that after the temperature reaches T_2 from 403 K, a decrease in ϵ' from the reference value ϵ'_{ref} occurs, and as the temperature changes from T_2 to T_1 ($T_1 > T_2$) at time t_2 the value of ϵ' approaches the reference value ϵ'_{ref} and then begins to decrease with increasing aging time after reaching the maximum. This relaxation behavior deviates from that observed for isothermal aging at T_2 .

In order to compare the change in ϵ' with the aging time for $t_w > t_2$, the data points for $t_w < t_2$ are removed and those

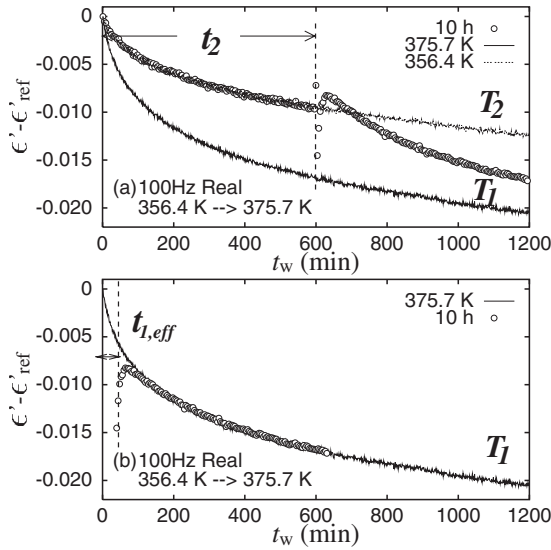


FIG. 1. (a) Difference between ϵ' and ϵ'_{ref} observed for the positive T -shift measurements. $T_1=375.7$ K and $T_2=356.4$ K ($\Delta T=19.3$ K). The data are obtained at 100 Hz. (b) $\epsilon' - \epsilon'_{ref}$ obtained by shifting the data points after the T shift in the negative direction of the time axis by τ_1 , so that the data points after the T shift are well overlapped with the standard relaxation curve at T_1 .

for $t_w > t_2$ are shifted to the negative direction of the t_w axis by a certain amount τ_1 so that the data points for $t_w > t_2$ can be well overlapped with those observed for the isothermal aging process after directly quenching from 403 K to T_1 , except for a small time region just after $t_w = t_2$. In this case, an effective time $t_{1,eff}$ can be obtained by the following relation:

$$t_{1,eff} = t_2 - \tau_1.$$

For the examples shown in Fig. 1, it is found that $t_{1,eff} = 0.6$ h, which means that the aging at $T_2=356.4$ K for a time $t_2=10$ h corresponds to the aging at $T_1=375.7$ K for a time $t_{1,eff}=0.6$ h. Figure 1(b) shows that the data points for $t_w > t_2$ can be well overlapped with the curve for T_1 after shifting by τ_1 , except for a small time region just after the temperature shift.

For a negative T shift from $T_1=375.7$ K to $T_2=356.4$ K, we can evaluate another effective temperature $t_{2,eff}$ in a manner similar to that for the positive T shift, as shown in Fig. 2(b). Here, the value of ϵ' is shown, which is shifted to the negative direction of the t_w axis by τ_2 . In this case, for a certain value of τ_2 , the data points at $t_w > t_1$ merge to the reference curve for the value of T_2 obtained above and thereafter lie on this curve. We can determine an effective time $t_{2,eff}$ as follows: $t_{2,eff} = t_1 - \tau_2$. Figure 2 indicates that $t_{2,eff} = 8$ h, which means that the aging at $T_1=375.7$ K for a time $t_1=10$ h corresponds to the aging at $T_2=356.4$ K for a time $t_{2,eff}=8$ h. Figure 2(b) shows that the data points for $t_w > t_1$ can be well overlapped with the curve for T_2 after shifting by τ_2 , except for a time region ($t_{2,eff} < t_w < 2t_{2,eff}$) after the temperature shift. The deviation of $\epsilon' - \epsilon'_{ref}$ from the reference curve at T_2 for the time range just after $t_{2,eff}$ in Fig. 2(b) will

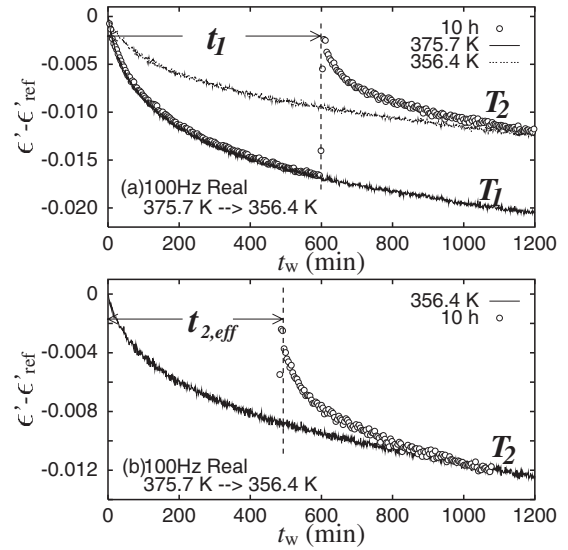


FIG. 2. (a) Difference between ϵ' and ϵ'_{ref} observed for the negative T -shift measurement from 375.7 K to 356.4 K. (b) $\epsilon' - \epsilon'_{ref}$ obtained by shifting the data points after the T shift in the negative direction of the time axis by τ_2 , in the same manner, as shown in Fig. 1(b).

be compared with that obtained in the spin glass and discussed later herein.

V. TWIN-T-SHIFT EXPERIMENTS

Figure 3 shows the real part of the ac-dielectric susceptibility at 100 Hz as a function of aging time after positive and negative temperature shifts with various values of t_1 (t_2) from 20 h to 1 h and $\Delta T=19.3$ K. The solid curves show the reference curve observed at T_1 (T_2) after quenching directly

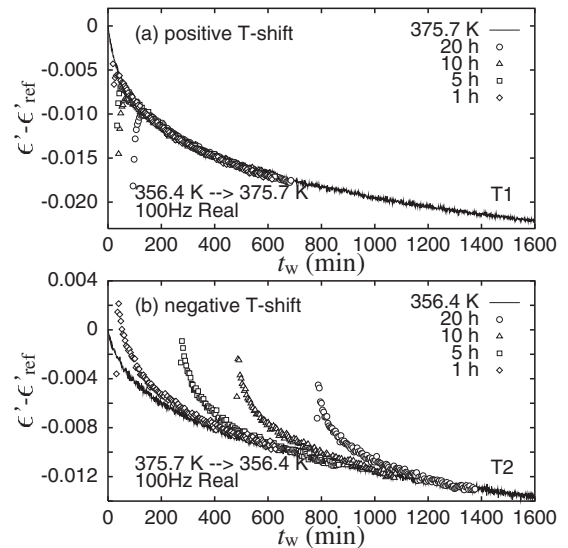


FIG. 3. (a) Values of $\epsilon' - \epsilon'_{ref}$ obtained by shifting the data points by a certain amount of time in order to obtain the effective aging times $t_{1,eff}$ (a) and $t_{2,eff}$ (b) for various aging times before the T shift. $\Delta T=19.3$ K.

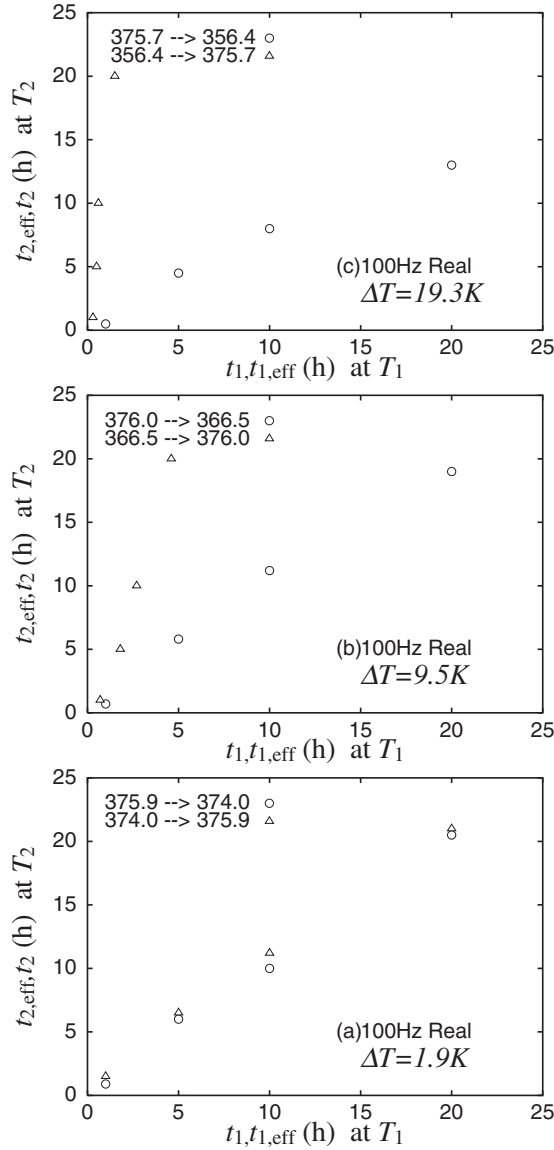


FIG. 4. Relation between t_w and t_{eff} in twin- T -shift experiments (T_1, T_2) and (T_2, T_1). $T_1 = 375.7 \text{ K}$ and $T_2 = T_1 - \Delta T$, where $\Delta T =$ (a) 1.9 K, (b) 9.5 K, and (c) 19.3 K. This figure shows that there is a crossover from cumulative aging to noncumulative aging with increasing ΔT . The data in this figure are evaluated based on the real part of the dielectric constant at 100 Hz.

from high temperature to the aging temperature. The data points are shifted in the negative direction of the t_w axis by a certain amount so that they will fall on top of the reference curve for T_1 (T_2). It is found that the effective aging times $t_{1,\text{eff}}$ ($t_{2,\text{eff}}$) increase with increasing aging times t_2 (t_1) at T_2 (T_1). From these results, we can extract the effective times as a function of aging time.

From a pair of negative and positive T -shift measurements, we obtain two effective times $t_{1,\text{eff}}$ and $t_{2,\text{eff}}$ as a function of aging times t_2 and t_1 , respectively. In Fig. 4 the horizontal axis is the time t_1 or $t_{1,\text{eff}}$ for T_1 and the vertical axis is the time $t_{2,\text{eff}}$ or t_2 for T_2 . The data points $(t_1, t_{2,\text{eff}})$ and $(t_{1,\text{eff}}, t_2)$ are plotted in Fig. 4 for various values of $\Delta T \equiv |T_1 - T_2|$. In Fig. 4(a), the data points for the negative T

shift fall on the same line as do the data points for the positive T shift for $\Delta T = 1.9 \text{ K}$. This suggests that the aging dynamics for $\Delta T = 1.9 \text{ K}$ obey a cumulative aging, where the contribution from the aging at T_1 to the coherent dynamic length scale and that from the aging at T_2 are totally additive, although the rate of aging dynamics differs depending on temperature. If ΔT increases from 1.9 K to 9.5 K and 19.3 K, it is clear that the data points obtained for the positive temperature shift do not fall on the same line as those for the negative temperature shift. This suggests that there is no reversibility between the positive and negative temperature shifts, and hence, the aging dynamics for $\Delta T = 9.5 \text{ K}$ and 19.3 K can be regarded as noncumulative aging. Therefore, there is a crossover from the cumulative aging to the noncumulative aging with increasing ΔT for aging dynamics in glassy states in PMMA.

VI. DISCUSSIONS

In order to further analyze the present data, a growth law of the dynamical coherent length $\ell_T(t)$ is required. This coherent length can be regarded as the linear size of the domain in which dipole moments are aligned in an orderly manner. Here, we assume that the growth of this ordered domain proceeds if the system exceeds a potential barrier $E(\ell)$, which is a function of the dynamic coherent length $\ell \equiv \ell_T(t)$, and that the following Arrhenius relation holds:

$$t = t_0 \exp\left(\frac{E(\ell)}{k_B T}\right),$$

where t is the elapsing time at temperature T , t_0 is a microscopic time scale, and k_B is the Boltzmann constant [2]. If the potential energy barrier is given by

$$E(\ell) = E_0 \left(\frac{\ell}{\ell_0}\right)^\psi,$$

where E_0 is a constant factor, ℓ_0 is the unit length, and ψ is a constant, we can obtain the following growth law of the ordered domain:

$$\ell_T(t) = \ell_0 \left[\frac{k_B T}{E_0} \ln\left(\frac{t}{t_0}\right) \right]^{1/\psi}.$$

Here, the scale dependence of the potential energy barrier can often be seen in problems of elastic objects, such as domain walls pinned by random impurities [2]. The constant factor E_0 can be dependent on temperature.

Next, we choose the parameters as follows: unit length $\ell_0 = 1$, exponent $\psi = 1$, and temperature unit $T_0 \equiv E_0/k_B = T_g$ (in this case, $T_g = 380 \text{ K}$ for PMMA). Using this growth law of the coherent length, we can convert both the aging time t_i and the corresponding effective time $t_{j,\text{eff}}$ into the domain sizes $\ell_{T_i}(t_i)$ or $\ell_{T_j}(t_{j,\text{eff}})$ ($i, j = 1$ or 2). For the positive T shift, we can obtain $(\ell_{T_1}(t_1), \ell_{T_2}(t_{2,\text{eff}}))$ from $(t_1, t_{2,\text{eff}})$, and for the negative T shift, we can obtain $(\ell_{T_2}(t_2), \ell_{T_1}(t_{1,\text{eff}}))$ from $(t_2, t_{1,\text{eff}})$.

Figure 5 shows the relation between $\ell_{T_i}(t_i)$ and $\ell_{T_j}(t_{j,\text{eff}})$ for the twin- T -shift experiments for three different values of

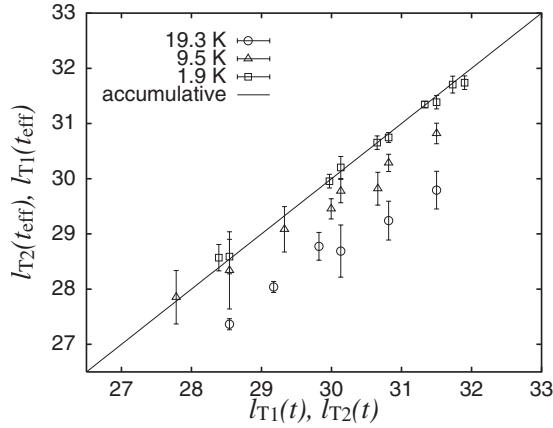


FIG. 5. Relationship between coherent length and effective coherent length obtained in the twin T -shift experiments for various values of ΔT (1.9 K, 9.5 K, and 19.3 K). The straight line indicates the case of cumulative aging. The error bars show the extent of data points for ac-electric fields of various frequencies (100 Hz, 1 kHz, and 10 kHz) and also for the choice of the real or imaginary parts of complex dielectric constant.

ΔT ($i, j=1$ or 2). The data points obtained from both the real and imaginary parts of the dielectric constant for three different frequencies of the applied electric field, 100 Hz, 1 kHz, and 10 kHz, are included. Error bars attached to the data points represent the variation for various conditions. The straight line corresponds to the case of fully cumulative aging. The results for $\Delta T=1.9$ K clearly show that the observed values fall on the line corresponding to the cumulative aging. However, as the values of ΔT increase from 1.9 K, the data points shown in Fig. 5 deviate from the straight line corresponding to the cumulative aging. Note also that, for a fixed value of ΔT , the data points fall on the same curve within error bars independent of whether the temperature shift is negative or positive or of which frequency is used for the capacitance measurements. This indicates that there is a unique coherent length for both the negative and positive T -shift measurements of the aging process.

Within the framework of the droplet theory, there is an overlap length $\ell_{\Delta T}$ for a given $\Delta T(=|T_1-T_2|)$ [19–22]. If the temperature-chaos effect exists, one can expect that the aging is totally uncorrelated between the two temperatures T_1 and T_2 for a length scale beyond $\ell_{\Delta T}$, while the aging can be regarded as cumulative for a length scale far below $\ell_{\Delta T}$. In spin glasses, the existence of the overlap length is one possible origin for the existence of the rejuvenation phenomenon [15]. In this case, we can expect that $\ell_{\text{eff}}(=l_{T_j}(t_{j,\text{eff}}))$ can be scaled as follows:

$$\frac{\ell_{\text{eff}}}{\ell_{\Delta T}} = f\left(\frac{\ell_{T_i}(t_{i,\text{eff}})}{\ell_{\Delta T}}\right),$$

where the scaling function $f(x)$ satisfies the relation $f(x)=x$ for $x \ll 1$ and $f(x)=1$ for $x \gg 1$ and $i, j=1$ or 2 [15]. This scaling function suggests that the coherent length cannot grow beyond the overlap length $\ell_{\Delta T}$, but it merges to $\ell_{\Delta T}$. In the present case, we assume that there is an overlap length

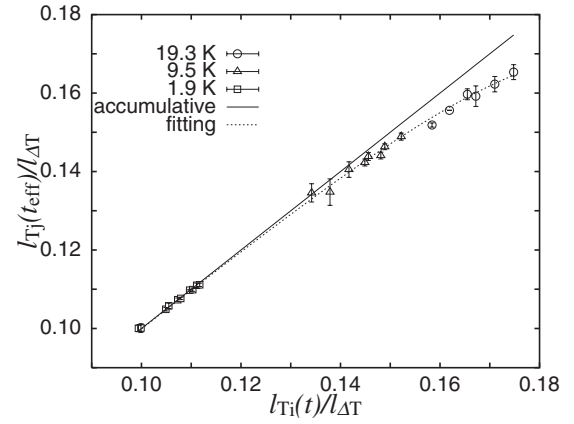


FIG. 6. Scaling behavior of the coherent length scale $\ell_T(t)$. Here, the overlap length is given by $\ell_{\Delta T}=\bar{\ell}|\frac{T_0}{\Delta T}|^\gamma$, where $\bar{\ell}=100$. The solid line corresponds to the case of cumulative aging. The dashed curve is for obtained data fitted with a model function.

scale $\ell_{\Delta T} \approx |\frac{T_0}{\Delta T}|^\gamma$ with the parameters $\ell_0=1$, $\gamma=0.2$, and $T_0=T_g=380$ K for PMMA. Then, we can obtain the scaling behavior of $\ell_{T_j}(t_{j,\text{eff}})$, as shown in Fig. 6. This scaling behavior is originally discussed for spin glass, and this scaling has been regarded as experimental evidence for the existence of the temperature-chaos effect.

The scaling behavior in Fig. 6, for the case of PMMA glass, suggests that the same argument based on the temperature chaos can be used for the existence of the rejuvenation phenomena, even in polymer glasses. This is very surprising if we take into account the large difference in structure between polymer glasses and spin glasses. In the literature, it has been reported that a temperature chaos can exist in polymer chains [23].

As shown in Figs. 1 and 2, after the positive T shift, the shifted dielectric susceptibility approaches the standard relaxation curve at T_1 from the lower side, whereas after the negative T shift, the shifted dielectric susceptibility approaches the standard relaxation curve at T_2 from the upper side. This behavior is observed in the nonequilibrium spin-glass dynamics of a strongly interacting ferromagnetic nanoparticle system (superspin glass), in which no evidence of temperature chaos or strong rejuvenation has been reported. Although the present results suggest the possibility of the existence of temperature chaos in polymer glasses, the above-described differences between spin glasses and polymer glasses should also be resolved in the near future.

Finally, the microscopic origin of the decrease in dielectric susceptibility should be discussed. In the case of PMMA, the dielectric susceptibility ϵ' (and ϵ'') decreases with aging time during the isothermal aging process [10,12]. This decrease can be observed also in other polymeric systems such as polycarbonate [24] and poly(ethylene terephthalate) [25]. Hence, the decrease in the dielectric susceptibility during isothermal aging process is a characteristic property common for physical aging of various polymeric systems, although the microscopic origin of this decrease is not fully understood.

It is well known that for many polymeric systems densification occurs due to physical aging. Hence, the density

should increase during the aging process and accordingly the dielectric strength $\Delta\epsilon$ should increase because $\Delta\epsilon$ is proportional to the number density of dipoles. Several dielectric measurements under high pressure for polymeric systems show an increase in dielectric constant upon high pressure [26–28]. In this case, it is expected that densification occurs, and hence the dielectric susceptibilities under high pressure might be compared to those during the aging process. However, the results under high pressure are opposite to those in our measurements. Therefore, there must be another physical origin which decreases the dielectric susceptibility and overcomes the densification.

During the course of physical aging two possible scenarios are possible: (i) Physical aging is probed well below the glass transition temperature, implying that the α process is totally frozen and only secondary relaxation processes, associated with localized motion, are dynamically active. In this case, orientational polarization associated with these processes would be reduced during physical aging. (ii) Physical aging is probed just below the glass transition temperature and the high-frequency tail of the α process is probed. In this latter case the decrease in the dielectric susceptibility is simply due to a shift of this tail to lower fre-

quency [29]. In the case of PMMA, there is a contribution from the β process below T_g which is associated with a localized motion of branches attached to polymer chains. Furthermore, measurements in the frequency domain of the dielectric loss clearly show that the peak frequency of the β process is not shifted, but the peak height decreases with increasing aging time without changing the shape of the dielectric spectrum during the isothermal aging process. The microscopic origin for the decrease in dielectric susceptibility in this case might be mainly attributed to the β process, not to the α process.

ACKNOWLEDGMENTS

The authors would like to thank H. Yoshino and H. Takayama for useful discussions. This work was supported by a Grant-in-Aid for Scientific Research (B) (No. 16340122) from the Japan Society for the Promotion of Science and also by KAKENHI (Grant-in-Aid for Scientific Research) on Priority Area “Soft Matter Physics” from the Ministry of Education, Culture, Sports, Science and Technology of Japan.

-
- [1] L. C. Struick, *Physical Aging in Amorphous Polymers and Other Materials* (Elsevier, New York, 1978).
 - [2] J.-P. Bouchaud, in *Soft and Fragile Matter*, edited by M. E. Cates and M. R. Evans (IOP, Bristol, 2000), p. 185.
 - [3] F. Lefloch, J. Hammann, M. Ocio, and E. Vincent, *Europhys. Lett.* **18**, 647 (1992).
 - [4] E. Vincent, J.-P. Bouchaud, J. Hamman, and F. Lefloch, *Philos. Mag. B* **71**, 489 (1995).
 - [5] K. Jonason, E. Vincent, J. Hammann, J. P. Bouchaud, and P. Nordblad, *Phys. Rev. Lett.* **81**, 3243 (1998).
 - [6] K. Jonason, P. Nordblad, E. Vincent, J. Hammann, and J. P. Bouchaud, *Eur. Phys. J. B* **13**, 99 (2000).
 - [7] P. Doussineau, T. de Lacerda-Aroso, and A. Levelut, *Europhys. Lett.* **46**, 401 (1999).
 - [8] R. L. Leheny and S. R. Nagel, *Phys. Rev. B* **57**, 5154 (1998).
 - [9] O. Kircher and R. Böhmer, *Eur. Phys. J. B* **26**, 329 (2002).
 - [10] L. Bellon, S. Ciliberto, and C. Laroche, *Eur. Phys. J. B* **25**, 223 (2002).
 - [11] L. Bellon, S. Ciliberto, and C. Laroche, e-print arXiv:cond-mat/9905160.
 - [12] K. Fukao and A. Sakamoto, *Phys. Rev. E* **71**, 041803 (2005).
 - [13] K. Fukao and H. Koizumi, *Eur. Phys. J. Special Topics* **141**, 199 (2007).
 - [14] L. Berthier and A. P. Young, *Phys. Rev. B* **71**, 214429 (2005).
 - [15] P. E. Jönsson, H. Yoshino, and P. Nordblad, *Phys. Rev. Lett.* **89**, 097201 (2002).
 - [16] K. Fukao and Y. Miyamoto, *Phys. Rev. E* **61**, 1743 (2000).
 - [17] K. Fukao and Y. Miyamoto, *Phys. Rev. E* **64**, 011803 (2001).
 - [18] K. Fukao, S. Uno, Y. Miyamoto, A. Hoshino, and H. Miyaji, *Phys. Rev. E* **64**, 051807 (2001).
 - [19] A. J. Bray and M. A. Moore, *Phys. Rev. Lett.* **58**, 57 (1987).
 - [20] D. S. Fisher and D. A. Huse, *Phys. Rev. B* **38**, 373 (1988).
 - [21] D. S. Fisher and D. A. Huse, *Phys. Rev. B* **38**, 386 (1988).
 - [22] D. S. Fisher and D. A. Huse, *Phys. Rev. B* **43**, 10728 (1991).
 - [23] M. Sales and H. Yoshino, *Phys. Rev. E* **65**, 066131 (2002).
 - [24] D. Cangialosi, M. Wübbenhorst, J. Groenewold, E. Mendes, H. Schut, A. van Veen, and S. J. Picken, *Phys. Rev. B* **70**, 224213 (2004).
 - [25] Elizabeth-Anne McGonigle, John H. Daly, Stephen D. Jenkins, John J. Liggat, and Richard A. Pethrick, *Macromolecules* **33**, 480 (2000).
 - [26] G. Floudas, C. Gravalides, T. Reisinger, and G. Wegner, *J. Chem. Phys.* **111**, 9847 (1999).
 - [27] K. Mpoukouvalas and G. Floudas, *Phys. Rev. E* **68**, 031801 (2003).
 - [28] G. Floudas, M. Mierzwa, and A. Schönhals, *Phys. Rev. E* **67**, 031705 (2003).
 - [29] P. Lunkenheimer, R. Wehn, U. Schneider, and A. Loidl, *Phys. Rev. Lett.* **95**, 055702 (2005).